

Synthesis Catalyst of Loading Nano Platinum on Graphene Nanosheets and Photodegradation of Bromophenol blue in Ultra-violet light.

Sanaa Tareq^{ID}✉, Souad A Mousa^{*ID}✉, Eman A Muhammed^{ID}✉

Department of Chemistry, College of Science for Women, University of Baghdad, Baghdad, Iraq.

*Corresponding Author.

Received 05/10/2023, Revised 14/04/2024, Accepted 15/04/2024, Published Online First 20/04/2024,
Published 01/11/2024



© 2022 The Author(s). Published by College of Science for Women, University of Baghdad.

This is an open-access article distributed under the terms of the [Creative Commons Attribution 4.0 International License](https://creativecommons.org/licenses/by/4.0/), which permits unrestricted use, distribution, and reproduction in any medium, provided the original work is properly cited.

Abstract

Nano Platinum was used as a new photocatalyst, which was loaded onto graphene for an effective photocatalyst under UV light used in dye photodegradation applications of dye as a common pollutant for water. Thus, platinum loaded on graphene (Pt/ GNS) catalyst was prepared by the sol immobilization method. The morphology of the synthetic photocatalyst has been characterized and investigated using a High-resolution Transmission electron microscope (HRTEM) and Energy Dispersive X-ray spectroscopy (EDX) attached to FESEM. By measuring the adsorption/adsorption N₂ using a Micrometrics surface analyzer, the Brunauer–Emmett–Teller (BET) surface areas of the photocatalysts were determined. The photocatalyst's crystalline structure was also examined using the Powder X-ray Diffraction (XRD) technique. Previously prepared catalysts have been examined under UV light as effective photocatalysts to degrade the bromophenol blue dye. The first step was the radiation of dye with no catalyst and the results show that there is demand for photocatalysts to make a reaction. The optimal values of Nano Platinum determined by the catalyst that was prepared by sol immobilization method. The effect of pH on the degradation reaction was measured, where it was specified that the basic media was the suitable media for the reaction.

Keywords: Bromophenol blue dye, Graphene, Kinetics, Photocatalyst, Photodegradation.

Introduction

Pollution of water by organic contaminants is a main environmental issue worldwide. The expansion of the industrial sector has led to an increase in the sources of water pollution, one of the most known contaminants are dyes¹⁻³. Wastewater produced from textile dyeing is considered a huge pollutant causing significant damage to the environment. Some dyes are insoluble in water and do not degrade ever, while dyes that exhibit solubility in water produce a toxic compound which are harmful to environments making it difficult to remove by traditional methods, as well as the intense color of aqueous solutions of

dyes inhibit the access of sunlight to the interior of the aqueous bodies⁴. There is a growing demand for the approach of low-cost techniques, as well as an interest in the development of environmentally friendly methods. Photocatalysis is a promising technique in environmental therapy that is currently under development⁴. There are several methods to reduce the contamination of dyes such as adsorption⁵⁻⁷, coagulation^{8,9}, filtration^{10,11}, and photodegradation¹²⁻¹⁴. It has been found that the photocatalytic degradation process is an interesting method because of its low cost, as well as because it

is a promising environmental technology¹⁵⁻¹⁷. Furthermore, various kinds of photocatalysts have been synthesized to degrade the effluents into less harmful materials^{18,19}. Bromophenol blue dye, also known as (3',3'',5',5''-Tetrabromophenolsulfonephthalein), which can be used as an industrial dye, an acid-base indicator and a biological stain. Photocatalysts were synthesized to study the photodegradation bromophenol and reduced in wastewaters.²⁰⁻²² Graphene is well-known as a monolayer of sp²-bonded carbon atoms into a

two-dimensional structure, it has been rapidly expanded interest of graphene due to its remarkable properties like high electronic and thermal conductivity, as well as features of transport and mechanical characteristics, in addition, it shows a very high surface area and the modification of textural properties of catalyst layers²³. In this work, the catalyst nano platinum on graphene nanosheets was synthesized and tested as photocatalyst as used a bromophenol as a case study.

Materials and Methods

Platinum (II) chloride [H₂PtCl₆·6H₂O] ((99.9% purity), sodium borohydride, polyvinyl-alcohol (PVA) with MW = 9,000-10,000 g/mol. 80% hydrolyzed), sodium tetrahydroborate, NaBH₄ (>96%), Hydrochloric acid baker analyzed™ A.C.S. reagent (98.08%) has been procured from J.T. Baker USA. The graphene used was 100 mesh particle size. Bromophenol blue (MW= 669.96) dye was supplied from HIMEDIA. Hydrochloric acid (36-37%) was provided from BDH and sodium hydroxide was procured from Riedel-De Haen AG Seelze-Hannover.

Synthesis of the Catalysts

Platinum was loaded on graphene. The catalyst of Pt/ GNS. prepared by sol immobilization method:

In this method, the required concentrations of aqueous solutions of PtCl₂ (Aldrich), first prepared using continuous stirring for 30 minutes at (2-3 rpm), then 1 g was prepared in 20 ml of polyvinyl alcohol added to the Pt mixture while continuing to stir for 5 minutes. The next addition was 0.1 m of NaBH₄ prepared at room temperature which was stirred for 30 minutes pending the color turning to dark brown. Thirty minutes after Sol was generated, the added graphene-supported material restrained the colloid formation. The pH of the solution was 1-3 and was controlled by adding hydrochloric acid with stirring settings²⁴. After 60 minutes, the slurry was separated and then washed off with water, and then the resulting substance was dried at 120° C for 16 hours. The produced catalyst using the sol immobilization technique was labeled as Pt/GNS SI.

Characterization

The characterization of the resulting catalysts was reviewed using multiple techniques. Field Emission Scanning Electron Microscopy (FESEM) has been used to detect the morphology of the prepared catalyst. Moreover, X-rays (EDX) and high-resolution transmission electron microscopy (HR-TEM) have shown energy-dispersing analysis.

The catalyst powder was dissolved in 99% high purity ethanol for sample preparation, where the suspension drop was vaporized on a preserved carbon permeable film using a TEM copper mesh continual through 300 mesh, and as well for Pt particle size by HRTEM (at 200 kV, in a JEOL 1200 EX, using CCD camera). The X-ray device (Model XRD 6000- Shimadzu) used a diffractometer with a monochromatic (Cu-Kα1) source working at 2.7 keV, and 40 mA, that is used in experimental configurations with (JCPDS) powder diffraction coil, and Cu K α radiation. Field emission scanning electron microscope.

Catalyst thermal analysis using the thermogravimetric analyzer (Mettler Toledo 990, TGA) (Pt crucibles, Pt / Pt- Rh thermocouple) was used to determine the total weight loss in the catalyst weight, and using N₂ gas for flushing with a heating rate of 10 °C min⁻¹, 30 mL. min⁻¹ a flow rate, and temperature ranged starting from room temperature to 1000° C. By N₂ adsorption/adsorption analyzer (micromeritics, 3-Flex, version 1.02) the surface area and pore size of the catalyst were determined by adopting the Brunauer Emmet-Teller (BET) method. To get rid of moisture and the rest of external gases on the external parts, the catalysts have been degassed at 200° C.

The desorption and adsorption of nitrogen on the catalysts were checked at -196°C . The acidity of catalyst was examined by temperature automated desorption using ammonia (TPD- NH_3); using a (Thermo-Finnigan TPD/R/O 1100) device equipped with a thermal-conductivity detector, TCD. NH_3 (2%) in helium was ramped for 60 min at $1^{\circ}\text{C min}^{-1}$. For 55 min, N_2 was flushed at room temperature to remove NH_3 in the gas phase. The programmed-temperature desorption was applied for evaluating the catalyst within a temperature range between 50 to 900°C .

Photocatalytic Measurements

As a photocatalyst, the performance of platinum supported by graphene nanoparticles was evaluated by performing a photodegradation test of bromophenol blue dye (BPB) under ultraviolet light (254 nm, 14 W) where a submerged lamp was used in the test solution, and different concentration of photocatalyst was added to 250 ml of 15 ppm of BPB dye solution with continuous steady stirring using a magnetic stirrer (wise) from Daihan Scientific. After exposing the draw samples (5 ml of solution) repeatedly to a light source every 5 minutes, the catalyst was removed from the solution using

centrifuge (800 Electric Centrifuge), then the absorbance of the bromophenol blue dye was measured at 591 nm by SmartSpecTM Plus spectrophotometer (BIO-RAD).

Absorption of BPB dye was converted to concentration using calibration curve, which was obtained by applying the beer-lambert relationship ($A = \epsilon b c$), when of various concentrations of BPB dye were prepared and measured their absorbance. A number of experiments have done frequently using different pH values, the pH of the solution had adjusted using sodium hydroxide (0.1M) and hydrochloric acid (0.1M), the pH values had measured using pH meter (Vernier @Go DirectTM Electrode Amplifier). The percentage of degradation of bromophenol blue dye was determined using the Eq. 1²⁵:

$$\begin{aligned} \text{Degradation \%} &= \frac{(C_0 - C_t)}{C_0} \\ &\times 100 \end{aligned} \quad 1$$

where C_0 and C_t are the initial concentration, and the concentration after UV irradiation.

Results and Discussion

Prepared catalyst characterization

EDX and HRTEM were used to characterize the morphology of the catalyst. platinum nanoparticles showed a high degree of uniformity diffused on the surface of the nanographene. The EDX analysis also showed signs for elements including carbon and oxygen, and presumably showing the Pt peaks of the resulting catalyst sample, which was associated with the successful loading of Pt on graphene. Also, the EDX analysis clearly showed strong signals for elemental copper that can arise from the carbon-plated copper grid that utilized in the analysis, and gold atoms at several energy levels essentially at 2.2 KeV and also at 9.8 KeV as shown in the Fig. 1²⁶.

It was confirmed that the Cu-Au alloy could produce high-quality copper-gold alloy nanotubes, that the elemental Au and Cu distribution ranges fully overlapped, and that the intensity in the outer layer was significantly higher than the intensity in the inner region, confirming the formation of Cu-Au alloy nanotubes.²⁷

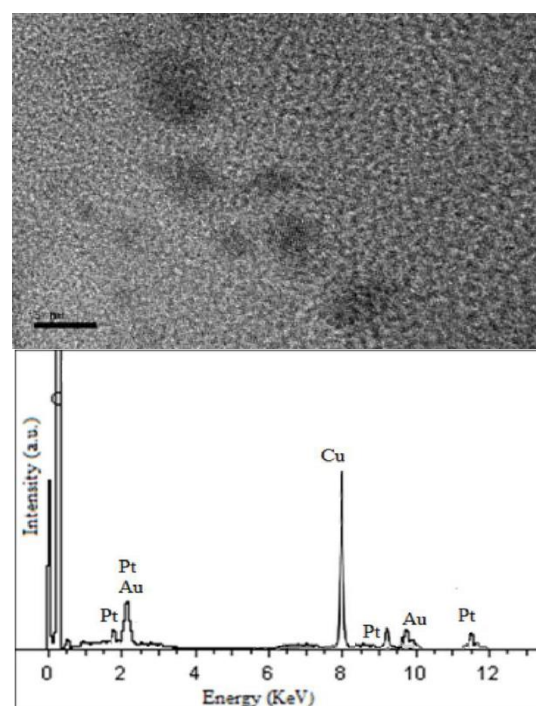


Figure 1. FESEM micrographs and EDX of the 5%Pt/GNS catalyst

The HRTEM technique used to assess the average size of platinum particles, as well as their distribution, dispersion, and function of Pt loading on Pt/GNS. The size distribution histogram of the metal nanoparticles in the catalyst was evaluated. More than 100 randomly selected particles were measured to obtain the Pt particle, platinum nanoparticle size of Pt/GNS is presented in Fig. 2.

Although the drying treatment took 24 hours at 120° C during the catalyst preparation process, the dispersion and distribution of the platinum nanoparticles on the graphene surface without aggregation appeared to be homogeneous and good enough according to HRTEM images. Due to the strong interaction between platinum and graphene molecules, the stability of platinum molecules on the graphene surface after heat treatment is relatively high in Fig. 2²⁸.

From Fig. 2, platinum particles with an average particle size of 5.7 nm distributed on graphene appear to be firmly gathered, while small platinum particles with a diameter in the range from 2 to 20 nm, are shown to be uniformly distributed on graphene sheets.

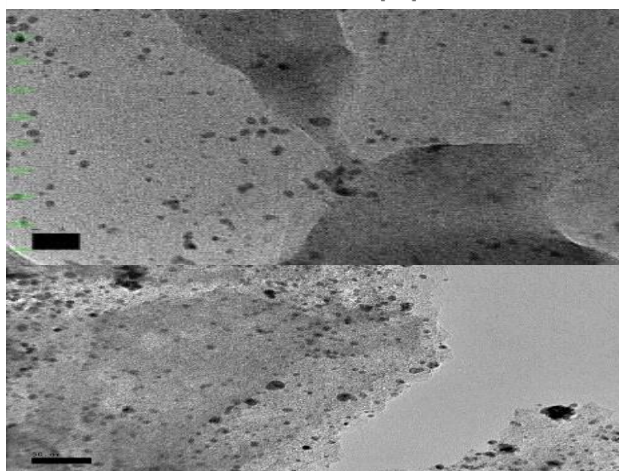
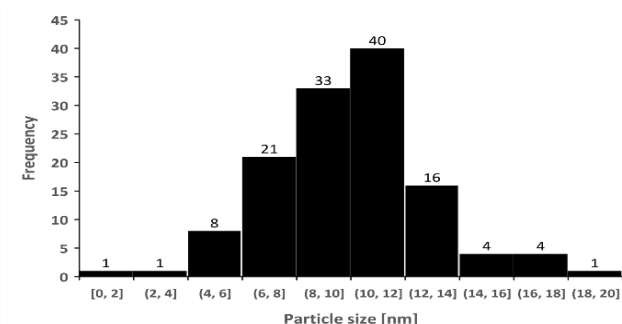


Figure 2. HRTEM micrographs and the compliant histograms of the particle size distributions for the 5%Pt/ GNS. specimen created using sol-immobilization technique, only dried at 120° C.

From Fig. 2, the HRTEM image of 5%Pt- GNS. that a uniform distribution of transparent GNS. nanoplates by platinum nanoparticles is visible enough and the assemblies appear to be quite few, signifying a strong interaction between GNS support and platinum particles. The average particle size of platinum nanoparticles was measured and estimated at 2.67 - 0.7 nm.

XRD Analysis

The supported catalyst's powder XRD patterns are shown in Fig. 3. It can be observed that face centered cubic (fcc) phase of platinum exhibits four diffraction peaks at 39.8, 46.3, and 67.7 that are referenced to the (1 1 1), (2 0 0), and (2 2 0) planes ²⁹.

The effect of chemical process performance during catalyst synthesis was observed by the appearance/disappearance of the diffraction peak (002) related to the interlayer spacing between the graphene nano nanoplates. Peak diffraction of catalysts appeared at 26.6, which is related to 200 planes of the hexagonal carbon lattice. It is clearly compatible with graphene in process conditions ³⁰. The average particle volume was calculated from half of the maximum full width of the peak (220) using the Shearer equation.²⁹

The average platinum particle sizes were estimated, which was 6, thus deducing that Pt-specific surface area is greater in graphene. The particle size of the supported Pt on graphene was relatively small, demonstrating that the unique structure and physical properties of graphene could have an assisting role in the distribution of Pt nanoparticles.

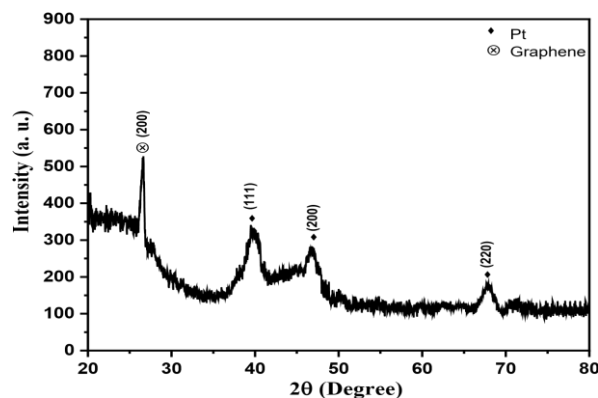


Figure 3. XRD patterns of the Pt/graphene catalyst.

The BET Surface area measurement of the surface area of the graphene nanosheets under nitrogen gas

absorption has been determined to be 67 ($S_{BET} / m^2 / g$), as well the measurement of the prepared catalyst 5% Pt/GNS was $113.1418 m^2/g$, whereas the BJH method has been applied to obtain Pore-size distribution of Pt/GNS and pore volume of the RGO to be 34.585 \AA and $0.518235 cm^3 g^{-1}$ respectively. It has been observed that there is an increase in the values of BET surface area (S_{BET}) of samples accompanied by increased loading of platinum on the surface of graphene. This increase in the surface area of the platinum/graphene photocatalyst will allow for higher activity sites for the photoreaction, facilitating the transfer of charge, and encouraging an increase in the performance of the photocatalytic reaction^{31,32}. Fig. 3 shows that the resulting Pt/GNS catalysts possess an isothermal type IV, which is microporous showing H_3 deceleration rings³³, and has been indicated to the presence of large amounts of medium pores and uniformly distribution of pore sizes, which belong to the isothermal type IV with a sharp increase at $P/P > 0.45$.

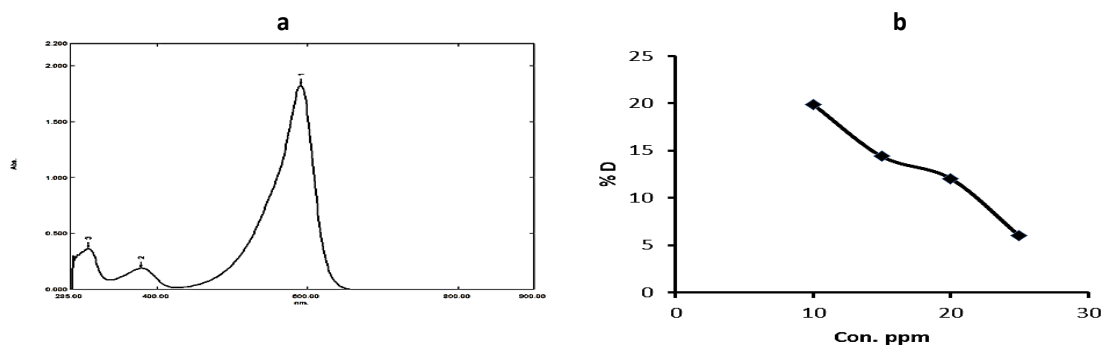


Figure 4.a Absorption spectrum of bromophenol blue dye, b) The relationship between D% of bromophenol blue dye solution and concentrations

Catalyst Concentration

In order to test the photocatalytic activity of the synthesized Graphene-Pt (Pt/GNS), different concentrations of synthesized Pt/GNS (0.005 - 0.025g) were added to aqueous solution of bromophenol dye at concentration (15 ppm) and irradiated under UV-light. Figure shows the results, it can be seen that the percentage of degradation increased, as the surface of catalyst is becoming available for the dye and water molecules to be absorbed, which undergo to attack by the generated of hydroxyl radicals. The optimal value of the photocatalyst Pt/GNS was recorded as (0.01 g / 250 ml of 15 ppm of BPB solution) when the degradation percentage was ($D\% \sim 79\%$).

Photodegradation of BPB

Fig. 4a shows absorption spectrum of bromophenol blue dye, the dye displays a chromophore peak at (248 nm) belonging to the dye's blue color, and the rest of three peaks displayed at 590 nm are associated with the dye's aromatic ring. Figure 4b shows the percentage of degradation (D%) of dye under UV-light without existing the catalyst Pt \ GNS at different concentrations of dye (10, 25, 15, and 20 ppm). It can be seen that the highest degradation percentage was 20% (D % 20% for 10 ppm). As the photodegradation processes depend on generating of hydroxyl radicals which has an essential role in degradation of dye, with existing of catalyst hydroxyl radicals were expected to be more. At the same time it can be seen from Fig. 4b that the photodegradation of bromophenol blue decreased as dye concentration increased, which means increasing the number of dye molecules leading to make the length of the path of photons entering the solution decreased³⁴.

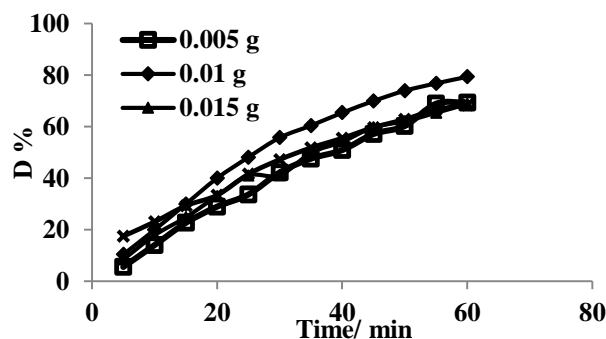


Figure 5. The relationship between contact time at different amounts of Pt-GNS and D% of bromophenol blue dye solution

H₂O₂ Effects

In this study, H₂O₂ was examined with Pt \ GNS to see if adding H₂O₂ to reaction mixture improved the powerful of Pt \ GNS as photocatalyst of BPB dye, the results are illustrated in Figure . In this case, the concentration of H₂O₂ was estimated to be 10 mM, and it was noticed from the results that the concentration of 10 mM was the best to degrade the dye using a catalyst amount (0.01 g / 250 ml) of Pt \ GNS under UV -light. The level of dye degradation has increased to about 90%. It has been concluded that hydrogen peroxide was an important parameter to add with the catalyst for dye degradation. Since free OH radicals produced by photolysis of H₂O₂ under ultraviolet light can react with dye molecules³⁵. In consideration of the fact that at high concentrations the solution undergoes self-quenching of OH• radicals by additional amounts of H₂O₂ to form HO₂• radicals, the concentration of H₂O₂ was kept at the appropriate dosage, so the degradation of dye reduced which can be due to the consumption of hydroxyl radicals OH• by H₂O₂ as briefed in following equations:

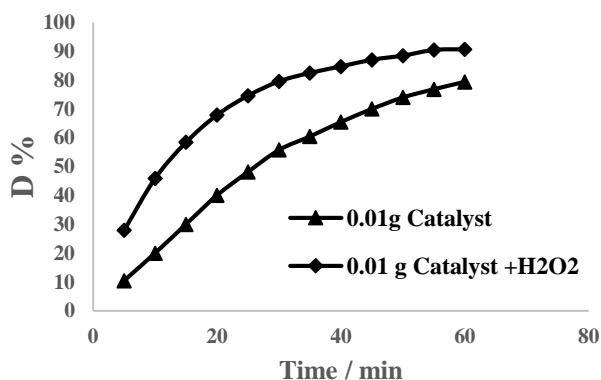
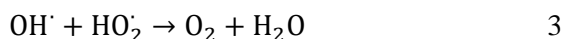


Figure 6. The relationship between D% and contact time at optimum value of photocatalyst ((0.01g/250 ml) of Pt\GNS) and (10 mM of H₂O₂).

Effect of pH

The photocatalytic activity of the synthesized Graphene-Pt (Pt\GNS) was examined at various media, where droplets of NaOH (0.1 M) and HCl (0.1

M) were added to adjust the pH of the dye solutions. The results of irradiation of BPB (15 ppm) under UV-light in acidic, basic and neutral media at pH (5.3, 7.5, and 11) in presence of (0.01g/250 ml) catalyst are shown in Figure , it can be noticed that there was an increase in percentage of degradation D% as long as there is an increase in the pH of the solution. The highest percentage of degradation was in basic media (11 pH). Enhancing dye degradation may be attributed to the increase the number of hydroxyl radicals at high pH, as well as changing in pH led to a change in the structure of BPB, which cause further interaction with radicals (O₂^{•-}; and OH[•])^{36,37}.

Figure shows the results of adding H₂O₂ to reaction mixture (dye and catalyst) at basic media (pH 11), it was found that the dye was completely degraded and the degradation percentage was 99% in 40 minutes, while other experiments needed an hour to decolorize the dye, it has been found that the results in this study are in agreement with the results in literatures, Table 1 shows photodegradation percentage (D %) of different photocatalysts comparing to the results in this study, which it can be indicated that the Pt \ GNS is an active as photocatalyst in degradation of bromophenol blue dye.^{38,39}

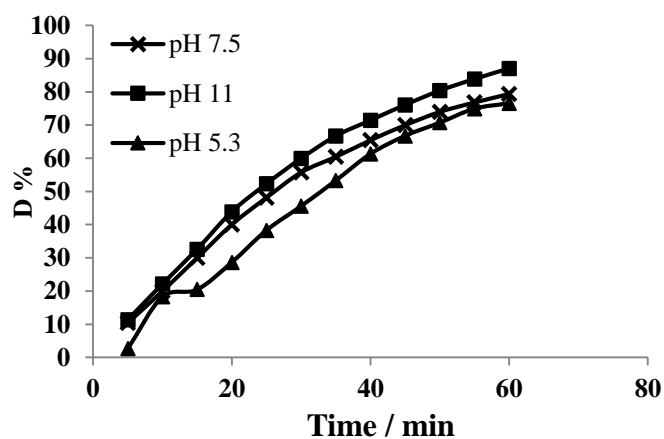


Figure 7. The relation between D% of Bromophenol blue dye solution and contact time at different media at (0.01g /250 ml) of Pt\GNS

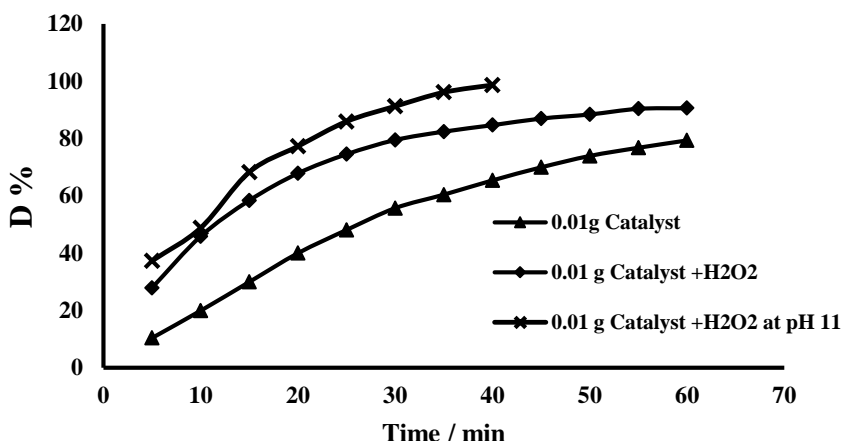


Figure 8. The relation between D% and contact time at (0.01g /250 ml) of Pt\GNS, ((0.01g /250 ml) of (Pt\GNS and 10 mM of H₂O₂) and ((0.01g /250 ml) of Pt\GNS,10 mM of H₂O₂ and at pH 11).

Table 1. Comparison of photodegradation percentage (D %) of different photocatalysts for Bromophenol blue dye

Catalyst	D%	Ref.
Nano Platinum on Graphene Nanosheets	79-99	This study
Graphene nanoplates-supported TiO ₂	79-95	35
Titanium dioxide-polypyrrole nanocomposites	97.53	37
S-SnO ₂	92.33	38
Parkia speciose Hassk pod extract	81.5-93.4	39
La ₂ O ₃	24.7-50.7	40

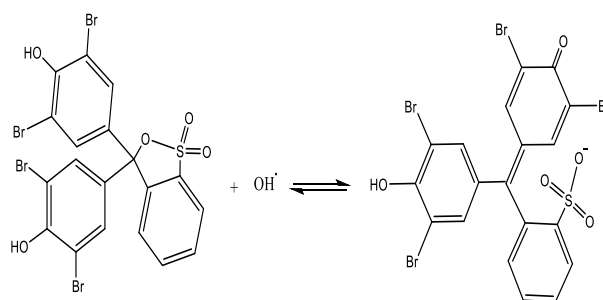


Figure 9. Possible mechanism of degradation of Bromophenol blue dye.

It was suggested that the possible mechanism to degrade of bromophenol blue included hydrolysis by presence of OH[·] as shown in Fig. 9 which finally degraded to CO₂ and H₂O.^{20,40}

Kinetics

The kinetics of the reaction was studied, the data was fitted to a first-order rate Eq. 2^{41,42}

$$\ln \frac{C_0}{C_t} = kt \quad 2$$

Where C₀ and C_t are concentration of dye before and after irradiation respectively, k is the rate constant, t is the irradiation time. Figure 10 displays the fitting curve; the rate constant value for the degradation of the dye was increased when using H₂O₂ and raised further at pH 11. Table 2 demonstrates the rate constant of the reaction and, R² values which describes that the data fit as a first-order reaction.

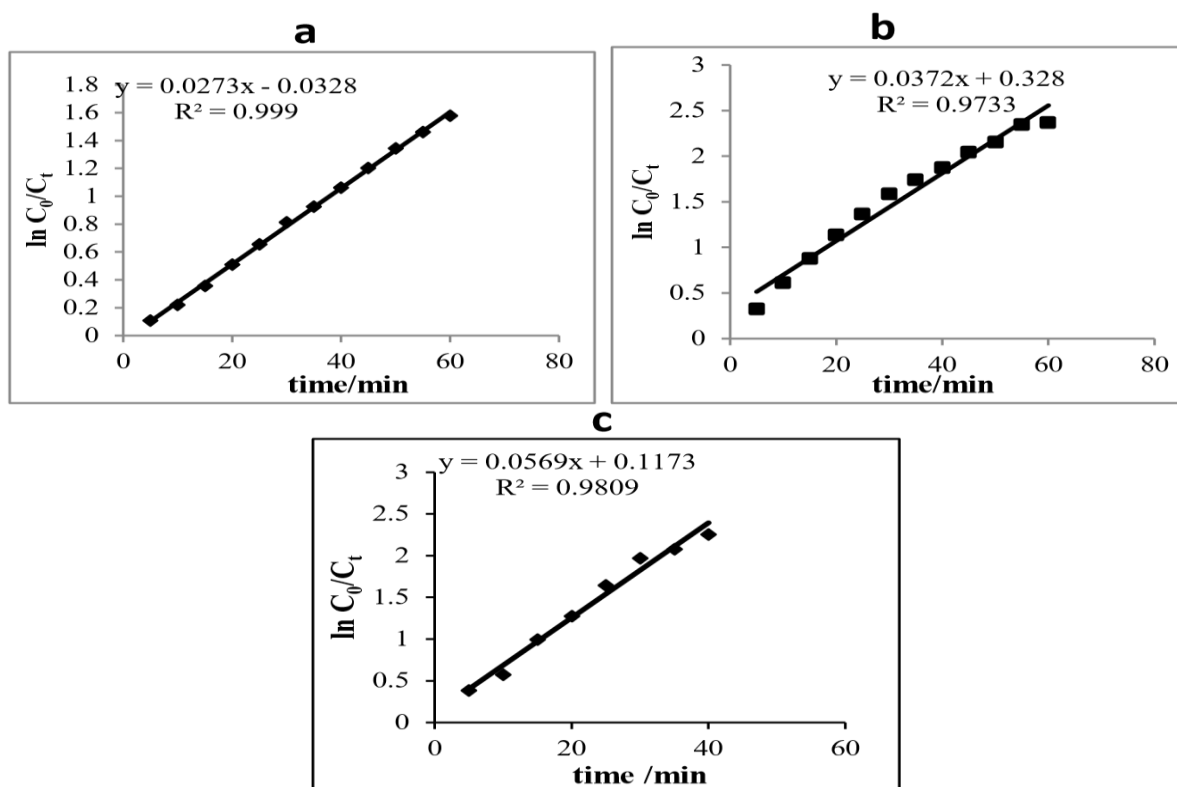


Figure 10. First order fit of Bromophenol blue dye at; a) (0.01g /250 ml) of Pt\GNS, b) ((0.01g /250 ml) of Pt\GNS and 10 mM of H₂O₂), c) ((0.01g /250 ml) of Pt\GNS,10 mM of H₂O₂ and at pH 11).

Table 2. rate constant of first order reaction and R² values

Condition	k/ min ⁻¹	R ²
0.01 g of Pt\GNS	0.0273	0.999
0.01 g of Pt\GNS and 10 mM of H ₂ O ₂	0.0372	0.9733
0.01 g of Pt\GNS + 10 mM of H ₂ O ₂ + pH 11	0.0569	0.9809

Conclusion

In this study, the catalyst of 5% Pt/GR was prepared by sol immobilization method and Pt nanoparticles on the Pt/ G were dispersed on the surface of graphene. The results showed using a High-resolution Transmission electron microscope (HRTEM). The dispersion and distribution were appropriate and homogeneous for platinum nanoparticles, which have an average particle size of 5.7nm distributed over graphene without aggregation due to the structure of the multi-layer graphene sheets as well as the high porosity of the graphene sheets. It enables the best mass transfer of dye and

nanometals as well as functional groups on graphene plates. Brunauer-Emmet-Teller (BET) has also been used to determine the surface area of the newly prepared catalyst displays.

The new product has been investigated using an x-ray diffraction (XRD) pattern. The synthetic catalyst Pt/ GNS was tested as a photocatalyst using bromophenol dye as case study. The degradation process has been done at various parameters; a dose of catalyst, media of reaction, and H₂O₂ effect.

Acknowledgment

The authors thank the Department of Chemistry in College of Science for Women for their

endless support and continuous help in completing this research.

Authors' Declaration

- Conflicts of Interest: None.
- We hereby confirm that all the Figures and Tables in the manuscript are ours. Furthermore, any Figures and images, that are not ours, have been included with the necessary permission for re-publication, which is attached to the manuscript.
- Ethical Clearance: The project was approved by the local ethical committee at University of Baghdad.
- Ethics statement:
No animal studies are present in the manuscript.
No human studies are present in the manuscript.
No potentially identified images or data are present in the manuscript.

Authors' Contributions Statement

S. T. contributed to conception, interpretation, analysis, revision and proofread of the presented manuscript. S. A. M. participated in design, acquisition of data, and drafting the manuscript. And

E. A. M. participated in acquisition of data. All authors discussed the results and contributed to the final manuscript.

References

1. Garg A, Chopra L. Dye Waste: A significant environmental hazard. *Mater Today Proc* .2022; 48: 1310-1315. <https://doi.org/10.1016/j.matpr.2021.09.003>
2. Alzain H, Kalimugogo V, Hussein K, Karkadan M. A Review of Environmental Impact of Azo Dyes. *Int J Res Rev*. 2023; 10(6): 673-689. <https://doi.org/10.52403/ijrr.20230682>
3. Lellis B, Fávoro-Polonio CZ, Pamphile JA, Polonio JC. Effects of textile dyes on health and the environment and bioremediation potential of living organisms. *Biotechnol Res Inn*. 2019; 3(2): 275-290. <https://doi.org/10.1016/j.biori.2019.09.001>
4. Saeed M, Muneerl M, Haq Au, Akram N. Photocatalysis: an effective tool for photodegradation of dyes—a review. *Environ Sci Pollut Res*. 2022; 29: 293–311. <https://doi.org/10.1007/s11356-021-16389-7>
5. Kadhim N, Mousa S, Muhammed E, Farhan A. A Comparative Study of the Adsorption of Crystal Violet Dye from Aqueous Solution on Rice Husk and Charcoal. *Baghdad Sci J*. 2020; 17: 295-304. [https://doi.org/10.21123/bsj.2020.17.1\(Suppl\).0295](https://doi.org/10.21123/bsj.2020.17.1(Suppl).0295)
6. Kweinor Tetteh E, Rathilal S. Adsorption and photocatalytic mineralization of bromophenol blue dye with TiO₂ modified with clinoptilolite/activated carbon. *Catalyst*. 2020; 11(1): 7. <https://doi.org/10.3390/catal11010007>
7. Ren L, Zhao G, Pan L, Chen B, Chen Y, Zhang Q , et al. Efficient removal of dye from wastewater without selectivity using activated carbon-Juncus effusus porous fibril composites. *ACS Appl Mater Interfaces*. 2021; 13(16): 19176-19186. <https://doi.org/10.1021/acsami.0c22104>
8. Hadadi A, Imessaoudene A, Bollinger J-C, Bouzaza A, Amrone A, Tahrooui H, et al. Aleppo pine seeds (Pinus halepensis Mill.) as a promising novel green coagulant for the removal of Congo red dye: Optimization via machine learning algorithm. *Environ Manag*. 2023; 331: 117286. <http://dx.doi.org/10.1016/j.jenvman.2023.117286>
9. Nnaji PC, Anadebe VC, Agu C, Ezemogu IG, Edeh JC, Ohanehi AA, et al. Statistical computation and artificial neural algorithm modeling for the treatment of dye wastewater using mucuna sloanei as coagulant and study of the generated sludge. *Rineng*. 2023; 19: 101216. <https://doi.org/10.1016/j.rineng.2023.101216>
10. Zhang J, Jiang F, Lu Y, Wei S, Xu H, Zhang J, et al. Lignin microparticles-reinforced cellulose filter paper for simultaneous removal of emulsified oils and dyes. *Int J Biol Macromol*. 2023; 230: 123120. <https://doi.org/10.1016/j.ijbiomac.2022.123120>
11. Cui Z, Wu J, Xu Y, Wu T, Li H, Li J, et al. In-situ growth of polyoxometalate-based metal-organic frameworks on wood as a promising dual-function filter for effective hazardous dye and iodine capture.

- Chem Eng J. 2023; 451: 138371. <https://doi.org/10.1016/j.cej.2022.138371>
12. Kumar A, Raorane CJ, Syed A, Bahkali AH, Elgorban AM, Raj V, et al. Synthesis of TiO₂, TiO₂/PANI, TiO₂/PANI/GO nanocomposites and photodegradation of anionic dyes Rose Bengal and thymol blue in visible light. *Environ Res.* 2023; 216 (3): 114741. <https://doi.org/10.1016/j.envres.2022.114741>
 13. Mousa SA, Tareq S, Muhammed EA. Studying the Photodegradation of Congo Red Dye from Aqueous Solutions Using Bimetallic Au-Pd/TiO₂ Photocatalyst. *Baghdad Sci.J.* 2021; 18(4): 1261. <https://doi.org/10.21123/bsj.2021.18.4.1261>
 14. Mousa SA, Tareq S, Muhammed EA, Kadhim MS. Synthesis of Bimetallic Au-Pt / TiO₂ Catalysts as an Efficient Catalyst for the Photodegradation of Crystal Violet Dye. *Baghdad Sci J.* 2021; 18(1): 0102. <https://doi.org/10.21123/bsj.2021.18.1.0102>
 15. Elanthikkal S, Mohamed HH, Alomair NA. Extraction of biosilica from date palm biomass ash and its application in photocatalysis. *Arab J Chem.* 2023; 16(3): 104522. <https://doi.org/10.1016/j.arabjc.2022.104522>
 16. Chabalala MB, Zikalala SA, Ndlovu L, Mamba G, Mamba BB, Nxumalo EN. A green synthetic approach for the morphological control of ZnO-Ag using β -cyclodextrin and honey for photocatalytic degradation of bromophenol blue. *Chem Eng Res Des.* 2023; 197: 307-322. <https://doi.org/10.1016/j.cherd.2023.07.029>
 17. Sharma K, Vaya D, Prasad G, Surolia P. Photocatalytic process for oily wastewater treatment: A review. *Int J Environ Sci Technol.* 2023; 20(4): 4615-4634. <http://dx.doi.org/10.1007/s13762-021-03874-2>
 18. Al-Nuaim MA, Alwasiti AA, Shnain ZY. The photocatalytic process in the treatment of polluted water. *Chem Pap.* 2023; 77(2): 677-701. <https://doi.org/10.1007/s11696-022-02468-7>
 19. Mousavi SM, Golestaneh M. Facile Synthesis of Fe/ZnO Hollow Spheres Nanostructures by Green Approach for the Photodegradation and Removal of Organic Dye Contaminants in Water. *J Nanostruct.* 2021; 11(1): 20-30. <https://doi.org/10.22052/JNS.2021.01.003>
 20. Cong Q, Ren M, Zhang T, Cheng F, Qu J. Efficient photoelectrocatalytic performance of β -cyclodextrin/graphene composite and effect of Cl⁻ in water: degradation for bromophenol blue as a case study. *RSC Adv.* 2021; 11(48): 29896-29905. <https://doi.org/10.1039/d1ra04533d>
 21. Khan Z, Ali F, Said A, Arif U, Khan K, Ali N, et al. Polyethylene glycol capped copper ferrite porous nanostructured materials for efficient photocatalytic degradation of bromophenol blue. *Environ Res.* 2022; 215: 114148. <https://doi.org/10.1016/j.envres.2022.114148>
 22. Moussaid D, Khallouk K, Moumnani FT, Fahoul Y, Tanji K, Barakat A, et al. High photocatalytic activity and stability of MnV₂O₆ and Mn₂V₂O₇ synthesized by simple low temperature method for bromophenol blue degradation. *J Photochem Photobiol A Chem.* 2023; 444: 114922. <https://doi.org/10.1016/j.jphotochem.2023.114922>
 23. Grigoriev S, Fateev V, Pushkarev A, Natalia AI, Valery NK, Mikhail Yu, et al. Reduced Graphene Oxide and Its Modifications as Catalyst Supports and Catalyst Layer Modifiers for PEMFC. *Mater.* 2018; 11: 1405. <https://doi.org/10.3390/ma11081405>
 24. Mousa SA, Tareq S, Muhammed EA. Studying the Photodegradation of Congo Red Dye from Aqueous Solutions Using Bimetallic Au - Pd / TiO₂ Photocatalyst. *Baghdad Sci J.* 2021; 18(2): 1261. <http://dx.doi.org/10.21123/bsj.2021.18.2.1261>
 25. Kisała J, Ferraria AM, Mitina N, Cieniek B, Krzeminski P, Pogocki D, et al. Photocatalytic activity of layered MoS₂ in the reductive degradation of bromophenol blue. *RSC adv.* 2022; 12(35): 22465-22475. <https://doi.org/10.1039/D2RA03362C>
 26. Hosny M, Fawzy M. Instantaneous phytosynthesis of gold nanoparticles via *Persicaria salicifolia* leaf extract, and their medical applications. *Adv Powder Technol.* 2021; 32(8): 2891-2904. <https://doi.org/10.1016/j.apt.2021.06.004>
 27. Jiang Z, Zhang Q, Zong C, Liu BJ, Ren B, Xie Z, et al. Cu-Au alloy nanotubes with five-fold twinned structure and their application in surface-enhanced Raman scattering. *Mater Chem.* 2012; 22(35): 18192-18197. <https://doi.org/10.1039/C2JM33863G>
 28. Yoo E, Okata T, Akita T, Kohyama M, Nakamura J, Honma I. Enhanced electrocatalytic activity of Pt subnanoclusters on graphene nanosheet surface. *Nano Lett.* 2009; 9(6): 2255-2259. <https://doi.org/10.1021/nl900397t>
 29. Chiang Y C, Liang C C, Chung, C P. Characterization of platinum nanoparticles deposited on functionalized graphene sheets. *Mater.* 2015; 8(9): 6484-6497. <https://doi.org/10.3390/ma8095318>
 30. Oyarce E, Roa K, Boulett A, Sotelo S, Cantero-Lopez P, Sanchez J, et al. Removal of dyes by polymer-enhanced ultrafiltration: an overview. *Polymers.* 2021; 13(19): 3450. <https://doi.org/10.3390/polym13193450>
 31. Novoselov KS, Geim AK, Morozov SV, Jiang D, Zhang Y, Dubonos SV, et al. Electric Field Effect in Atomically Thin Carbon Films. *Science.* 2004; 306(5696): 666-669. <https://doi.org/10.1126/science.1102896>
 32. Fini A, Breccia A. Chemistry by microwaves. *Pure Appl Chem.* 1999; 71(4): 573-579. <https://doi.org/10.1351/pac199971040573>
 33. Ullah K, Ye S, Zhu L, Jo SB, Jang WK, Cho KY, et al. Noble metal doped graphene nanocomposites and its study of photocatalytic hydrogen evolution. *Solid State Sci.* 2014; 31: 91-98. <https://doi.org/10.1016/j.solidstatesciences.2014.03.006>

34. Shah T, Gul T, Saeed K. Photodegradation of bromophenol blue in aqueous medium using graphene nanoplates-supported TiO₂. *Appl Water Sci* 2019; 9(4): 1-7. <https://doi.org/10.1007/s13201-019-0983-z>
35. Rauf MA, Ashraf S, Alhadrami SN. Photolytic oxidation of coomassie brilliant blue with H₂O₂. *Dyes Pigm.* 2005; 66(3): 197-200. <https://doi.org/10.1016/j.dyepig.2004.09.006>
36. Buenviaje SC, Usman KS, Payawan L M. Synthesis and characterization of titanium dioxide-polypyrrole nanocomposites for the photodegradation of bromophenol blue. *AIP Conf Proc.* 2018; 1958: 020015. <https://doi.org/10.1063/1.5034546>
37. Sani KI, Umar G, Hamisu A. Synthesis of Visible Light Response S-SnO₂ Catalyst for Optimized Photodegradation of Bromophenol Blue. *JPCFM.* 2021; 4(2): 22-33. <https://doi.org/10.54565/jphcfum.1008388>
38. Fatimah I, Pratiwi EZ, Wicaksono WP. Synthesis of magnetic nanoparticles using *Parkia speciosa* Hassk pod extract and photocatalytic activity for Bromophenol blue degradation. *Egypt J Aquat Res.* 2020; 46(1): 35-40. <https://doi.org/10.1016/j.ejar.2020.01.001>
39. Farrukh M, Imran F, Ali S, Khaleeq-ur-Rahman M, Naqvi I. Micelle assisted synthesis of La₂O₃ nanoparticles and their applications in photodegradation of bromophenol blue. *Russ J Appl Chem.* 2015; 88: 1523-1527. <https://doi.org/10.1134/S1070427215090220>
40. Azmat R, Khalid Z, Haroon M, Mehar KP. Spectral Analysis of Catalytic Oxidation and Degradation of Bromophenol Blue at Low pH with Potassium Dichromate. *Adv Nat Sci.* 2013; 6: 38-43. <https://doi.org/10.3968/j.ans.1715787020130603.1628>
41. Nawaz A, Atif M, Khan A, Siddique M, Ali N, Naz F, et al. Solar light driven degradation of textile dye contaminants for wastewater treatment – studies of novel polycationic selenide photocatalyst and process optimization by response surface methodology desirability factor. *Chemosphere.* 2023; 328: 138476. <https://doi.org/10.1016/j.chemosphere.2023.138476>
42. Effiong J F, Nyong AE, Boekom EJ, Simon N. Photocatalytic Degradation and Kinetics of Dyes in Textile Effluent Using UV – ZnO-Al System. *Asian J Appl Chem Res.* 2023; 13 (2): 23-32. <https://doi.org/10.9734/ajacr/2023/v13i2240>

تصنيع المحفز المحضر من تحميل دقائق النانوية للبلاتين على سطح الكرافين والتجزئة الضوئية لصبغة البروموفينول الأزرق تحت الأشعة فوق البنفسجية

سناء طارق ، سعاد عبد موسى ، ايمان عدنان محمد

قسم الكيمياء، كلية العلوم للبنات، جامعة بغداد، بغداد، العراق.

الخلاصة

تم في هذا البحث استخدام المحفز الجديد المصنع من تحميل دقائق البلاتين النانوية على سطح الصفائح النانوية للكرافين كمحفز ضوئي واختباره لدراسة التجزئة الضوئية لملوثات المياه وازالتها بشكل نهائي من مصادر المياه لما لها من تأثير سلبي على البيئة. حيث تم استخدام صبغة البروموفينول الأزرق كمثال على أحد الملوثات. في البدء تم التأكد من تحضير المحفز بالطريقة المستخدمة في طريقة العمل من خلال تشخيصه باستخدام عدد من التقنيات ومنها تقنية المجهر الإلكتروني النافذ عالي الدقة، تقنية طاقة تشتت الأشعة السينية الطيفي عن طريق قياس الامتزاز/ الامتزاز باستخدام غاز النتروجين. كذلك تم قياس المساحة السطحية للمحفز المصنع، بالإضافة الى فحص التركيب الكريستال للمحفز باستخدام تقنية حيود الأشعة السينية. وبعد ان تم التأكد من التركيب النهائي للمحفز الضوئي تضمن الجزء الثاني من العمل دراسة قدرة المحفز المصنع على استخدامه في التجزئة الضوئية لصبغة البروموفينول الأزرق تحت الأشعة فوق البنفسجية حيث تم تحضير عدة تراكيز من صبغة البروموفينول الأزرق، تم تشييع الصبغة بدون وجود المحفز ووجد بان التجزئة الضوئية لم تكن فعالة وبعد ذلك تم استخدام المحفز مع المحلول المائي للصبغة وبتركيز 15 جزء من المليون وأجريت التجارب باستخدام عدة اوزان من المحفز لتحديد افضل وزن يمكن استخدامه من المحفز في كمية محددة من محلول الصبغة ووجد ان 0.01 غرام من الصبغة لكل 250 مليلتر من المحلول المائي للصبغة هو افضل نسبة يمكن الحصول عليها. كما تم اختبار الوسط للتفاعل في الوسطين الحامضي والقاعدي ووجد ان تفكك الصبغة يزداد بشكل ملحوظ في الوسط القاعدي. تم اقتراح ميكانيكية التفاعل التي بينت ان تكون الجذور الحرة لها دور كبير في مهاجمة الاواصر المزدوجة في الصبغة.

الكلمات المفتاحية: البروموفينول الأزرق، التجزئة الضوئية، الحركية، الكرافين، المحفز الضوئي.